doi:10.1016/j.jmb.2004.05.007 *J. Mol. Biol.* (2004) **340**, 891–907

JMB

Available online at www.sciencedirect.com

SCIENCE DIRECT®

ELSEVIER

Biochemical and Structural Studies of the Interaction of Cdc37 with Hsp90

Wei Zhang[1], Miriam Hirshberg[1], Stephen H. McLaughlin[2] Greg A. Lazar[1], J. Günter Grossmann[3], Peter R. Nielsen[1] Frank Sobott[2], Carol V. Robinson[2], Sophie E. Jackson[2]* and Ernest D. Laue[1]*

[1]*Department of Biochemistry University of Cambridge Tennis Court Road Cambridge CB2 1GA, UK*

[2]*Cambridge University Chemical Laboratory Lensfield Road, Cambridge CB2 1EW, UK*

[3]*Synchrotron Radiation Department, CCLRC Daresbury Laboratory Daresbury, Warrington WA4 4AD, UK*

**Corresponding authors*

The heat shock protein Hsp90 plays a key, but poorly understood role in the folding, assembly and activation of a large number of signal transduction molecules, in particular kinases and steroid hormone receptors. In carrying out these functions Hsp90 hydrolyses ATP as it cycles between ADP- and ATP-bound forms, and this ATPase activity is regulated by the transient association with a variety of co-chaperones. Cdc37 is one such co-chaperone protein that also has a role in client protein recognition, in that it is required for Hsp90-dependent folding and activation of a particular group of protein kinases. These include the cyclin-dependent kinases (Cdk) 4/6 and Cdk9, Raf-1, Akt and many others. Here, the biochemical details of the interaction of human Hsp90β and Cdc37 have been characterised. Small angle X-ray scattering (SAXS) was then used to study the solution structure of Hsp90 and its complexes with Cdc37. The results suggest a model for the interaction of Cdc37 with Hsp90, whereby a Cdc37 dimer binds the two N-terminal domain/linker regions in an Hsp90 dimer, fixing them in a single conformation that is presumably suitable for client protein recognition.

Keywords: molecular chaperone; heat shock protein; kinase; protein–protein interaction; ATPase activity

Introduction

The molecular chaperone Hsp90 is required for the folding, assembly and activation of a large number of signal transduction molecules, in particular kinases and steroid hormone receptors.[1–4] For both its *in vivo* and *in vitro* function Hsp90 needs to bind and hydrolyse ATP[5–8] and this ATPase activity is regulated, in part, by the transient association of Hsp90 with a variety of co-chaperones,[9–13] as well as by the binding of client proteins.[10]

In Hsp90-dependent folding processes tetratricopeptide repeat (TPR)-domain containing co-chaperones, which bind to the Hsp90 C-terminal MEEVD motif,[14] are well-documented modulators of Hsp90 ATPase activity.[9,10,13] For example, the TPR-domain protein Hop,[15] known as Sti1 in yeast,[16] binds to both Hsp70 and Hsp90 *via* such domains, acting as an adaptor to transfer the client protein from Hsp70 to Hsp90.[15] As a result of the binding of Hop to Hsp90, the ATPase activity of yeast Hsp90 is suppressed and this is thought to favour client protein loading onto Hsp90.[9] Interestingly, human Hop has little effect on the ATPase activity of human Hsp90. However, it strongly inhibits the ATPase activity in the presence of a client-protein.[10] Recent work has shown that Sti1/Hop binds to the first 24 amino acid residues of Hsp90 thereby preventing interactions between the two N-terminal domains in an Hsp90 dimer,

Present addresses: G. A. Lazar, Xencor, Inc., Monrovia, CA 91016, USA; M. Hirshberg, Department of Human Microbiology, Sackler School of Medicine, Tel Aviv University, Tel Aviv 69978, Israel.

Abbreviations used: SEC, size-exclusion chromatography; AUC, analytical ultracentrifugation; SAXS, small-angle X-ray scattering; GA, geldanamycin; TPR, tetratricopeptide repeat.

E-mail addresses of the corresponding authors: sej13@cam.ac.uk; e.d.laue@bioc.cam.ac.uk

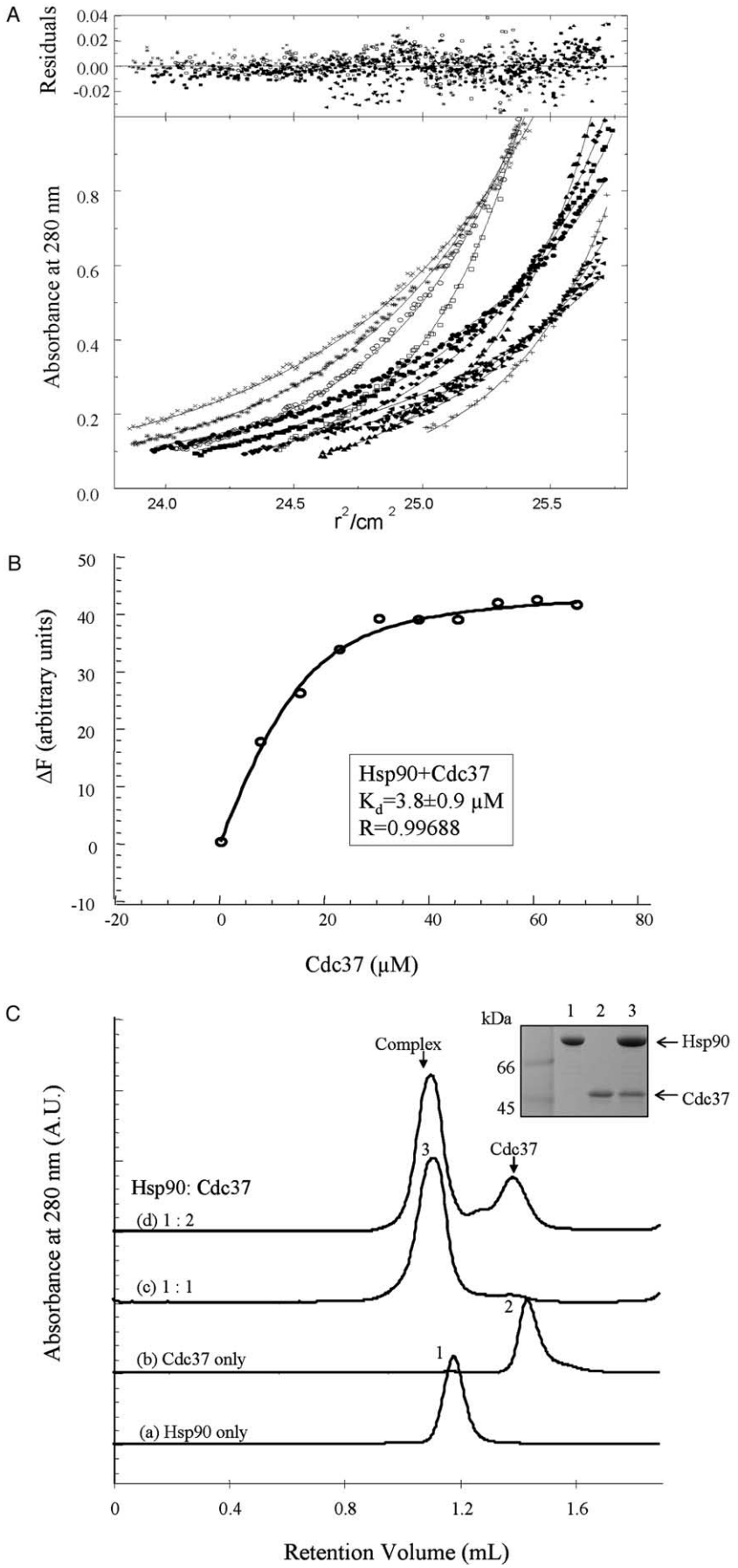

Figure 1 (*legend opposite*)

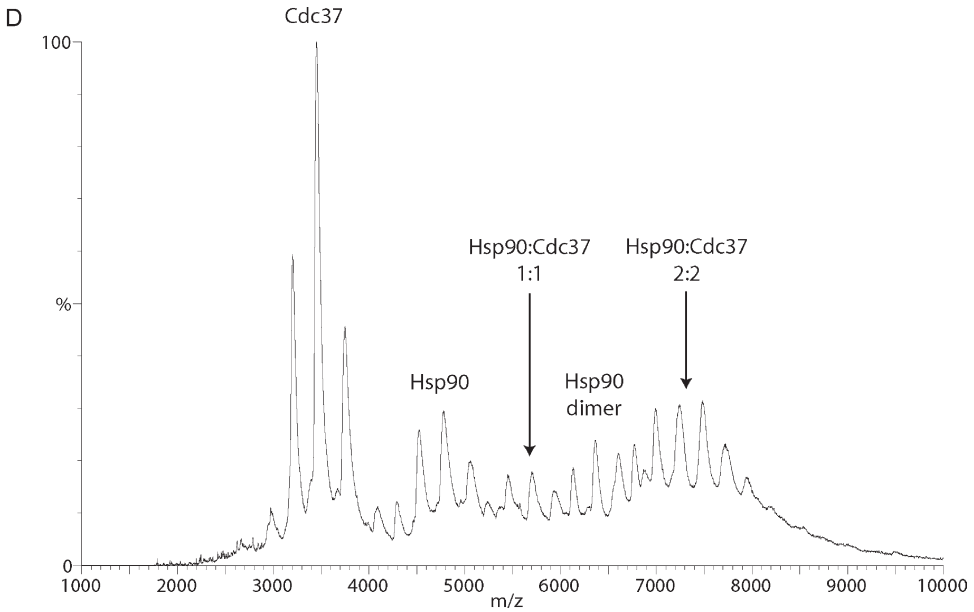

Figure 1. Characterisation of the oligomeric state of Cdc37 and its stoichiometry of binding to Hsp90. A, Sedimentation equilibrium analysis of Cdc37. The lower panel shows the three protein concentrations 1: A_{280} 0.2 at (◀) 13,200 rpm, (▼) 14,500 rpm, (►) 16,700 rpm, and (+) 18,700 rpm. 2: A_{280} 0.3 at (●) 13,200 rpm, (■) 14,500 rpm, (◆) 16,000 rpm, and (▲) 18,700 rpm. 3: A_{280} 0.5 at (×) 13,200 rpm, (*) 14,500 rpm, (○) 16,000 rpm, and (□) 18,700 rpm. The continuous lines show the curves calculated using the parameters obtained by least squares fitting. The upper panel shows the residuals left when subtracting the calculated values from the measured points. B, Determination of the K_d for the Cdc37–Hsp90 interaction using fluorescence spectroscopy. The change in fluorescence at 340 nm upon Hsp90–Cdc37 complex formation with increasing Cdc37 concentrations was fitted to equation (1) (see Materials and Methods) to obtain the dissociation constant. C, Analysis of the Cdc37–Hsp90 interaction using size exclusion chromatography. Hsp90 and Cdc37 either alone or as a mixture were incubated on ice for one hour before separation on a Superdex 200 PC 3.5/30 analytical gel filtration column. The protein elution was monitored by absorbance at 280 nm: Hsp90 alone (a), Cdc37 alone (b), the mixture of Hsp90 and Cdc37 at a 1:1 molar ratio (c) and Hsp90 and Cdc37 mixed at a 1:2 molar ratio (d). Inset: SDS-PAGE analysis of the protein(s) in each of the eluted peaks. Lane 1, peak from trace (a); lane 2, peak from trace (b) and lane 3, peak from trace (c). D, NanoESI spectrum of the Hsp90-Cdc37 complex at 2.5 mg/ml in 1 M aqueous ammonium acetate buffer (pH 7.0). Data was acquired on a Micromass LCT time-of-flight mass spectrometer at an elevated source pressure of 8mbar and cone voltage of 200 V.

which is thought to be important for ATP hydrolysis.[13] In contrast to Hop, the TPR-containing immunophilin, FKBP52, has little effect on the basal ATPase activity and may even increase the rate of ATP turnover when a client protein is bound.[10]

In addition, other co-chaperones that do not possess a TPR-domain, have also been shown to regulate the rate of ATP turnover by Hsp90. In particular, the small acidic protein p23 inhibits both the basal and client-protein stimulated ATPase activity.[10] Recently, a new co-chaperone, Aha1, was discovered and shown to be an activator of the Hsp90 ATPase activity in yeast.[11] Thus, it is clear that the ATPase activity of Hsp90 is strongly regulated by co-chaperones and client proteins supporting the evidence that shows that ATP binding and hydrolysis are critical steps in the function of Hsp90 in activating kinases and other client proteins. Exactly how co-chaperones regulate the ATPase activity of Hsp90 and how ATP binding and hydrolysis drive conformational changes in the chaperone system, which leads to the activation of client proteins, is not, however, known.

Cdc37 is a heat shock protein and co-chaperone that is required for Hsp90-dependent folding and activation of particular protein kinases.[17] A broad range of kinases that form complexes with Hsp90 and Cdc37 have now been identified, e.g. cyclin-dependent kinases (Cdk) 4/6 and Cdk9,[18–21] Raf-1,[22,23] Akt[24] and the list continues to lengthen†. Recently, Hsp90/Cdc37-dependent client proteins have been reported that are not kinases, including the androgen receptor and hepadnavirus reverse transcriptase.[25,26] However, kinases still represent the majority of Cdc37 client proteins and Cdc37 is specifically required for the recruitment of protein kinases into complexes with Hsp90. Whether Cdc37 first binds to kinase substrates and directs them to Hsp90, as was originally proposed, or whether it binds to Hsp90 thereby altering its substrate specificity is still unclear. Cdc37 and Hsp90 might also jointly recognise the substrate.

Unlike Hop and the Hsp90-associated immunophilins, Cdc37 does not contain TPR motifs and, therefore, does not bind to the C-terminal MEEVD

† See http://www.picard.ch/DP/downloads/downloads.html for an up-to-date list

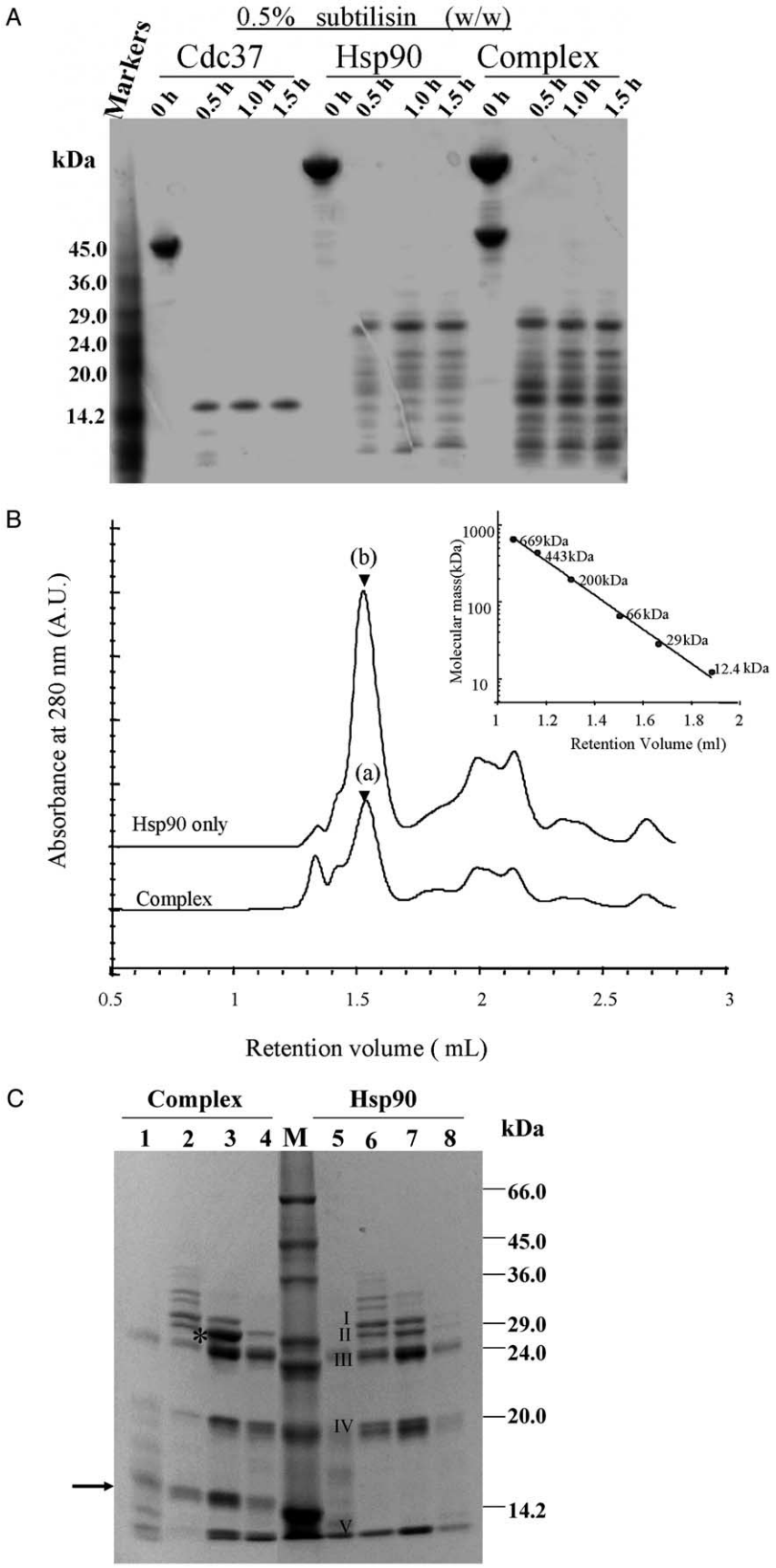

Figure 2. Identification of the binding domains of Cdc37 and Hsp90. A, Time-course of limited proteolysis of purified Cdc37, Hsp90 and the Cdc37–Hsp90 complex with Subtilisin. Undigested samples containing equal amounts of enzyme-free buffer were taken at zero hour as controls. Proteolytic fragments were subsequently separated on a 4–12% NuPAGE gel and stained with Coomassie Brilliant Blue. B, Separation of proteolytic fragments of Hsp90 and

motif in Hsp90. Although Cdc37's precise role in Hsp90 function remains unclear, the direct interaction of Cdc37 with Hsp90 is necessary for client protein–Hsp90 interactions. For example, Cdc37 enhances the association of Hsp90 with its client kinases both *in vitro* and *in vivo*,[23,27,28] and a truncated mutant of Cdc37 that cannot bind to Hsp90 reduces the affinity of client kinases for Hsp90.[3,23,29] Moreover, Cdc37–Hsp90 interactions do not simply provide a passive structural bridge for passing the client protein substrate to Hsp90: it also participates intimately in the folding process.[28] For example, it suppresses the ATPase activity of Hsp90, possibly modulating ATP turnover during the client protein loading phase.[12] Recently, the role of Cdc37 has become more complex with the discovery that it has several Hsp90-independent functions, including the ability to interact with other co-chaperones in the absence of Hsp90 and the ability to support yeast growth and protein folding without its Hsp90-binding domain.[17,30]

Cdc37 forms a basal complex with Hsp90 in the absence of client protein,[12,28,31] that is salt labile and unaffected by the presence of the Hsp90 ATPase inhibitor geldanamycin (GA).[12,28,29] Domain mapping of Cdc37 indicated that the N-terminal half is required for binding the kinase,[23,29,31] whilst the C-terminal half is necessary for interaction with Hsp90[23,29] and suppression of its ATPase activity.[12] Based on the sequence similarity between Cdc37 and Harc, a relative of Cdc37, the Hsp90-binding domain has been proposed to be within a 120 amino acid residue segment in the central region of Cdc37.[32]

A number of studies have attempted to identify the Cdc37-binding domain in Hsp90, providing inconsistent results. For example, an early study based on the observation that the TPR protein Hop competes with the binding of Cdc37 to Hsp90, proposed that Cdc37 binds to the C-terminal region of Hsp90 adjacent to the TPR-domain binding site.[33] However, more recently another study showed that a new member of the Hsp90 protein family, Hsp90N, which lacks an N-terminal domain and most of the adjacent charged linker sequence, fails to interact with Cdc37 although the middle and C-terminal domains remain intact.[34] Here, the biochemical properties of the interaction of human Hsp90β and Cdc37 have been characterised. The results suggest a model for the interaction of Cdc37 with Hsp90, whereby a Cdc37 dimer binds the two N-terminal domain/linker regions in an Hsp90 dimer, fixing them in a single conformation. This model explains why the C-terminal domain of Hsp90 enhances the binding of Cdc37. Moreover, it also explains why the binding of Cdc37 inhibits the ATPase activity of Hsp90.

Results

Although it has been known for many years that human Hsp90 interacts with its co-chaperone Cdc37 in complexes with particular client proteins, the biochemical properties of this interaction have not so far been clearly characterised. In order to study the interaction of these chaperones in more detail, the full-length human Hsp90β and human Cdc37 proteins were generated by expression in *Escherichia coli* and purified to 99% homogeneity.

The oligomeric state of Cdc37 and stoichiometry of binding to Hsp90

Previous studies have shown that the dimerisation region in Hsp90 is located in a C-terminal domain.[35,36] In order to gain insight into the self-association state of Cdc37, size-exclusion chromatography (SEC) and analytical ultracentrifugation (AUC) were employed. SEC analysis showed that the molecular mass of Cdc37 is approximately 100 kDa, approximately double that of the theoretical mass of a single molecule (~45 kDa, data not shown). In addition, sedimentation equilibrium AUC was employed to determine the oligomeric state of Cdc37. The experiment was performed, using different initial loading concentrations of Cdc37, at four rotor speeds, providing 12 data sets. Analysis of these data sets showed that the simplest model that is consistent with the data is a mixture of a monomer and a homo-dimer with a dissociation constant, K_d, of ~80(±20) μM (Figure 1A). We note that this value is somewhat higher than that determined.[12]

In vitro, the binding of Hsp90 to Cdc37 is readily disrupted by high salt concentrations, and the interaction between the two chaperones tightened by formation of a ternary complex with a client protein.[28] Here, we determined the binding affinity

the Hsp90–Cdc37 complex on an analytical Superdex 200 PC 3.2/30 gel filtration column at 4 °C. Samples were cleaved with 0.5% (w/w) of Subtilisin at room temperature for 1.5 hours and immediately separated. The major absorbance peak of proteolysed complex and Hsp90 are indicated, (a) and (b), respectively. Inset: the log of the molecular mass of the calibration proteins against their retention volume (ml) was fitted using linear regression. The calibration proteins used were: thyroglobulin (669 kDa), apoferritin (443 kDa), β-amylase (200 kDa), bovine serum albumin (66 kDa), carbonic anhydrase (29 kDa) and cytochrome *c* (12.4 kDa). C, SDS-PAGE analysis of SEC separated proteolysis products. Lanes 1–4, proteolytic fragments in peak fractions across peak (a) above, from digestion of the Cdc37–Hsp90 complex. Lanes 5–8, proteolytic fragments in peak fractions across peak (b) above, from digestion of Hsp90 alone. Lane M, molecular mass markers. The arrow indicates the Hsp90-binding domain of Cdc37. The asterisk marks an Hsp90 band in lane 3 which is protected in the digestion of the complex.

of the two proteins *in vitro* (high protein, low salt concentrations) using the intrinsic tryptophan fluorescence of Cdc37: the K_d for the interaction of Cdc37 with Hsp90 was determined to be 3.8(±0.9) μM (Figure 1B). This value is similar to that determined previously using CD spectroscopy.[12]

The stoichiometry of binding of Cdc37 to Hsp90 was next analysed by SEC studies, which suggested that a single Cdc37/Hsp90 complex is formed when the two proteins are mixed at a 1 to 1 molar ratio, but that free Cdc37 is observed when the two proteins are mixed with an excess of Cdc37 (Figure 1C). This critical result was confirmed by native-state mass spectrometry studies in which Cdc37 was seen to bind as a dimer to an Hsp90 dimer, there being a much weaker signal corresponding to a monomer of Cdc37 binding to the Hsp90 monomer (Figure 1D).

The central region of Cdc37 is a structured Hsp90-binding domain

A series of earlier studies have indicated that fragments comprising the middle and C-terminal regions of Cdc37 have the ability to bind Hsp90.[23,29,31] To determine the precise binding domains on both proteins, the Hsp90/Cdc37 complex formed *in vitro* was subjected to limited proteolysis to reveal the structured regions of the two proteins in the complex. A non-specific protease, Subtilisin, was used to digest the complex and the isolated Cdc37 and Hsp90 proteins were also digested in parallel as controls. Using 0.5% (w/w) enzyme at room temperature, Cdc37 was digested down from a 45 kDa molecule into a small fragment of less than 16 kDa after approximately 30 minutes. Interestingly, this 16 kDa fragment remained stable after 1.5 hours digestion (Figure 2A). This result implies that there is a very stable and highly structured 16 kDa domain (about one third of the protein), while the remainder of the protein is either unstructured or structured but susceptible to proteolysis. It was further determined by N-terminal sequencing and mass spectrometry analysis that the stable fragment comprises 130 residues (Lys147-Lys276) in the central region of Cdc37. This domain is hereafter referred to as Cdc37c.

In contrast to Cdc37, Hsp90 has a more stable structure as multiple fragments survive even after 1.5 hours of digestion with Subtilisin (Figure 2A). Formation of a complex between Cdc37 and Hsp90 might have been expected to change the digestion profile of either protein, though in practice it was difficult to ascertain which bands showed enhanced protection from digestion (Figure 2A). To address this issue, SEC was used to separate the digested products based on their size-related mobility and to monitor which fragment(s) co-elute with each other by sodium dodecyl sulphate-polyacrylamide gel electrophoresis (SDS-PAGE). Digested complex and digested Hsp90 fragments were analysed under the same conditions, where the latter was used as a control. In this comparison the digestion of the complex can again be seen to be similar to that of Hsp90 (Figure 2B). The components of the two main peaks were identified by SDS-PAGE and Coomassie blue staining. This analysis showed that a band with a similar mass to that of Cdc37c was present in the major peak of the digested complex, but absent from that of Hsp90 digested alone (Figure 2C); subsequently, this fragment was shown by N-terminal sequencing to be Cdc37c. Because both major peaks elute at a retention volume of about 1.5 ml, equivalent to a molecular mass of ~66 kDa using the standard linear calibration curve (Figure 2B inset), this result shows that Cdc37c was bound to an Hsp90 fragment

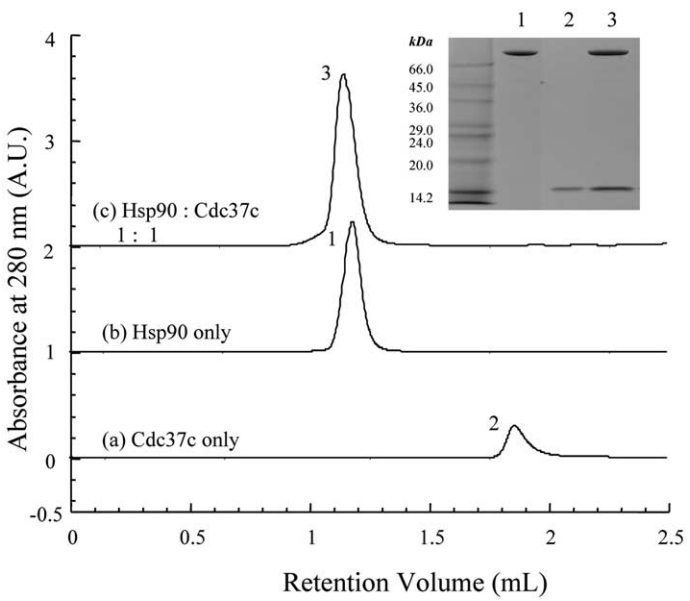

Figure 3. Analysis of the Cdc37c–Hsp90 interaction by SEC. Hsp90 and Cdc37c either alone or mixed at a one to one molar ratio were incubated on ice for one hour before separation on a Superdex 200 PC 3.5/30 analytical column. The protein elution was monitored by absorbance at 280 nm: Cdc37c alone (a); Hsp90 alone (b); the mixture of Hsp90 and Cdc37c (c). Inset: SDS-PAGE analysis of the protein(s) in each peak. Lane 1, trace (b); lane 2, trace (a) and lane 3, trace (c).

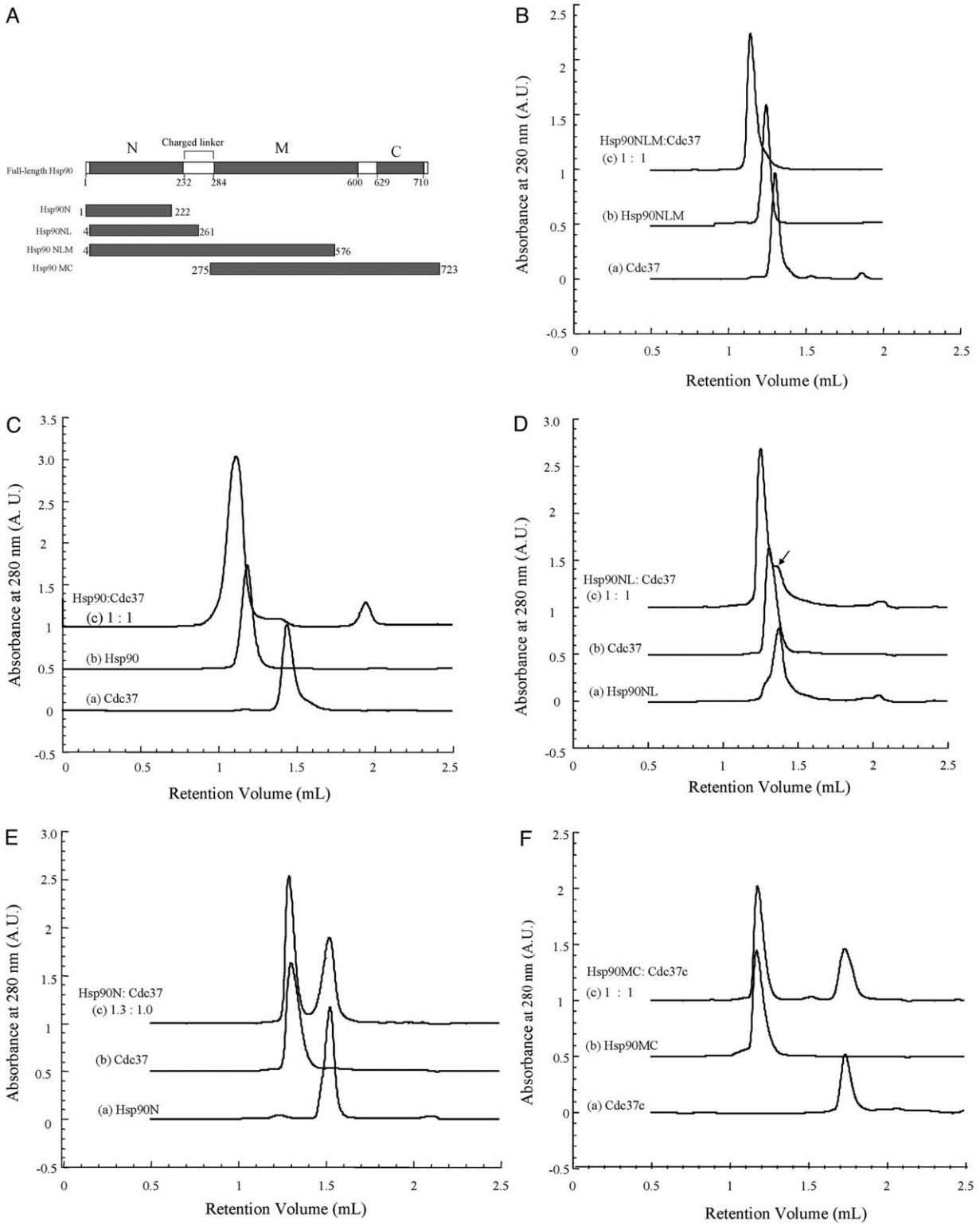

Figure 4. Analysis of the interaction of either full-length and truncated variants of Hsp90 with Cdc37 by SEC. Individual proteins and mixtures at a final protein concentration of 150 μM were incubated for one hour on ice prior to separation on a Superdex S200 PC 3.2/30 analytical column. The elution of proteins was monitored by absorbance at 280 nm. A, Schematic diagram illustrating the full-length and truncated versions of Hsp90 generated here. The nomenclature of the three structural domains in the full-length protein is that adopted by Stebbins *et al*.[39] B, The absorbance traces of Cdc37 alone (a); Hsp90NLM alone (b); and a mixture of Cdc37 and Hsp90NLM at an equal molar ratio (c). C, The absorbance trace of Cdc37 alone (a); Hsp90 alone (b); and a mixture of Cdc37 and Hsp90 at an equal molar ratio (c). D, The absorbance traces of Hsp90NL alone (a); Cdc37 alone (b); and a mixture of Hsp90NL and Cdc37 at an equal molar ratio (c). The arrow indicates the peak corresponding to free Hsp90NL. E, The absorbance traces of Hsp90N alone (a); Cdc37 alone (b); and a mixture of Hsp90N and Cdc37 at 1.3 to 1.0 molar ratio (c). F, The absorbance trace of Cdc37c alone (a); Hsp90MC alone (b); and a mixture of Cdc37c and Hsp90MC at an equal molar ratio (c).

when eluted from the column (the identification of this fragment is discussed below).

To further confirm that Cdc37c is the Hsp90-binding domain, this fragment was generated by DNA cloning and the protein expressed in *E. coli*. As judged by SEC analysis Cdc37c binds full-length Hsp90 to form a complex when mixed in a 1 to 1 molar ratio (Figure 3). As can be clearly seen, isolated Cdc37c is absent from the mixture, suggesting that Cdc37c binds to Hsp90 in a stoichiometric fashion. Taken together, the results presented here demonstrate that Cdc37c is the Hsp90-binding domain. In addition, estimation of the molecular mass of Cdc37c from the SEC analysis suggests that, unlike the intact Cdc37 protein, this Hsp90-binding fragment is monomeric in solution (see calibration in Figure 2B).

The minimal Cdc37-binding domain in Hsp90 comprises the N-terminal domain plus charged linker region

Structural and biochemical studies have shown that Hsp90 consists of three structural domains, where the N-terminal and middle domains are connected by a flexible charged linker.[37–41] The limited proteolysis studies in Figure 2 showed that the same five Hsp90 fragments were formed both in the presence and absence of Cdc37c (Figure 2C, lanes 3 and 7, indicated by letters I–V). However, only one fragment, that marked with an asterisk in Figure 2C, was more abundant in the digestion of the complex than in the Hsp90 control, suggesting that this fragment is protected in the complex with Cdc37. The identity of this fragment (along with the other four) was assigned by N-terminal sequencing and its overall mass. The protected fragment starts at Val4, and given its mass of ~29 kDa (from SDS-PAGE) we estimated that it included both the N-terminal domain and the charged linker of Hsp90. (The other four fragments were similarly assigned to the middle domain of Hsp90.)

To further investigate the Cdc37-binding region on Hsp90, the N-terminal domain plus the charged linker of Hsp90, together with several other truncated fragments, were generated by expression in *E. coli*. A schematic diagram of the different truncated constructs is shown in Figure 4A. One of these, Hsp90NL, a fragment which comprises the N-terminal domain plus the charged linker region of Hsp90 (Val4-Gly261), migrated at a mass of ~29 kDa by SDS-PAGE (data not shown), similar to the mass of the identified limited proteolysis fragment (see above).

The interaction of Cdc37 was studied with the N-terminal domain of Hsp90 alone (Hsp90N; residues Pro1-Lys222); with Hsp90NL (as discussed above); with a construct comprising the N-terminal domain, linker region and middle domain (Hsp90NLM; residues Val4-Lys576); and with a middle domain, C-terminal domain construct (Hsp90MC; residues Tyr275-Asp723). Figure 4 shows the SEC profiles of mixtures of the different constructs with Cdc37, all at the same concentration (150 μM). As shown in Figure 4B, from a comparison of Hsp90NLM alone (trace b), Cdc37 alone (trace a) and Hsp90NLM mixed with an equal molar ratio of Cdc37 (trace c), it can be seen that a single almost symmetrical peak appears for the mixture with a smaller retention volume than for Hsp90NLM. This demonstrates that all of the protein mixture forms a complex when mixed at an equi-molar ratio under these conditions. A similar result was obtained with full-length Hsp90 and Cdc37 (Figure 4C).

A mixture of Hsp90NL and Cdc37 formed under the same conditions (Figure 4D, trace c) can also be seen to produce a peak with a shorter retention volume and increased absorbance than with either protein alone, suggesting that a complex is formed by these two proteins. However, the peak is not symmetric and the shoulder indicates that the complex is breaking down to the free components during the gel filtration experiment. The interaction of Hsp90N and Cdc37 is shown in Figure 4E. Notably, the trace of the mixture of Hsp90N with Cdc37 (Figure 4E, trace c) has two peaks, which are similar to those of the two individual proteins (traces a and b), apart from the fact that the peak corresponding to Hsp90N is slightly smaller and the peak corresponding to Cdc37 is slightly larger. However, the retention volumes are the same and the results suggest that any binding between these two components is weak. Because we observed that Hsp90NL forms a weaker complex with Cdc37 in comparison to either Hsp90NLM or full-length Hsp90, we also investigated whether the middle and C-terminal domains contained a second binding interface for the interaction. To this end, the interaction of Hsp90MC with Cdc37 was also studied. However, it can be clearly seen in Figure 4F that the SEC trace of the mixture of Hsp90MC with Cdc37c (trace c) is identical to those of the individual proteins (traces a plus b).

Overall, the results from the SEC analysis presented in Figure 4 suggest that Hsp90NL comprises the smallest fragment that is sufficient for binding Cdc37, i.e. that both the N-terminal and charged linker region are required for interaction of Cdc37 with Hsp90. This conclusion is consistent with the finding from the limited proteolysis experiments, in which a fragment comprising the Hsp90 N-terminal domain and charged linker region is protected from digestion (Figure 2C). However, the results also reveal that the middle/C-terminal domains of Hsp90 play a role in enhancing the interaction.

The N-terminal domain of Hsp90 is sufficient for binding Cdc37c

The limited proteolysis experiments presented in Figure 2 revealed that Cdc37c is the Hsp90-binding domain. We also, therefore, carried out similar SEC

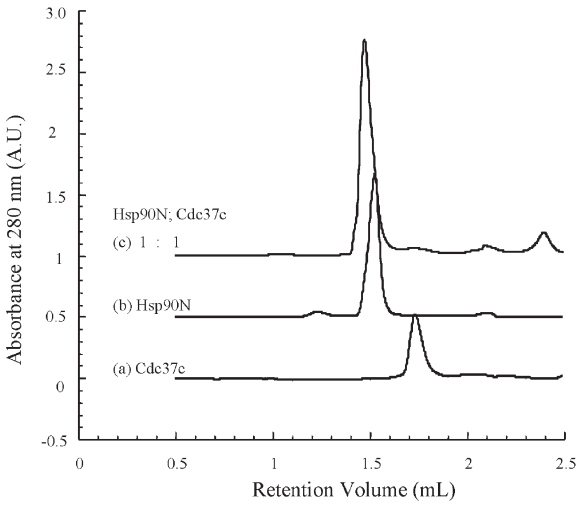

Figure 5. Analysis of the Hsp90N–Cdc37c interaction using SEC. Purified recombinant Hsp90N and Cdc37c were mixed and incubated prior to separation on a Superdex S200 P.C. 3.2/30 column. The absorbance traces are Cdc37c alone (a); Hsp90N alone (b); and a mixture of Hsp90N and Cdc37c at an equal molar ratio (c).

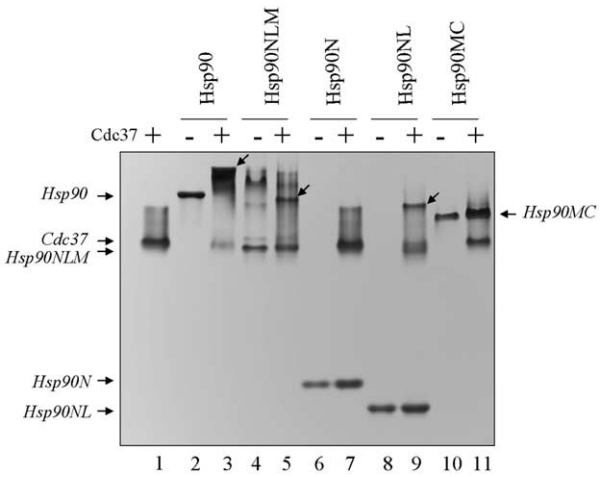

Figure 6. Analysis of the interaction of Cdc37 with either full-length Hsp90 or its truncated variants by non-denaturing (native) PAGE. Cdc37 (70 μM) was mixed with an equal molar ratio of either the full-length or truncated versions of Hsp90 and incubated in a Tris–HCl buffer (pH 8.0), containing fresh 2 mM DTT on ice for one hour. Either 2 μl of the individual proteins (70 μM) or 4 μl of the mixture (70 μM) were loaded on to a 14% Tris–Glycine gel (Novex) and run under non-denaturing condition as described in Materials and Methods. The gel was stained with Coomassie Brilliant Blue. Lane 1, Cdc37. Lanes 2, 4, 6, 8 and 10, either full-length or truncated versions of Hsp90 (−). Lanes 3, 5, 7, 9 and 11, either full-length or truncated versions of Hsp90 mixed with an equal molar ratio of Cdc37 (+). The bands corresponding to complexes are indicated by arrows (lanes 3, 5 and 9).

experiments for Cdc37c to those described above for full-length Cdc37. Surprisingly, these showed that Cdc37c is able to bind to Hsp90N, the isolated N-terminal domain of Hsp90 (Figure 5). This result is in marked contrast to the minimal or weak binding of full-length Cdc37. As expected, Cdc37c also formed complete complexes with both Hsp90NL and Hsp90NLM under the same conditions (data not shown). These results illustrate that Cdc37c has a much stronger binding capacity toward the N-terminal domain of Hsp90 than does the full-length Cdc37. This suggests that the binding of Cdc37 to Hsp90 is in some way hindered by the remainder of the molecule.

The middle and C-terminal domains of Hsp90 cannot direct interactions with Cdc37, but enhance the binding

Further support for the conclusions drawn from the SEC results and additional insight into the interaction was obtained through use of a non-denaturing gel electrophoresis assay, in which Cdc37 was incubated with the same quantities of full-length or truncated variants of Hsp90. Figure 6 shows that full-length Cdc37 and Hsp90 almost completely form a complex (lane 3). Among the truncated variants, Hsp90NLM and Hsp90NL partially associate with Cdc37 (indicated by arrows in lanes 5 and 9), whilst neither Hsp90N nor Hsp90MC show any sign of interaction with Cdc37. It should be noted that these experiments were carried out at lower protein concentrations than in the SEC analysis (see Materials and Methods). Thus, weak binding of two proteins, e.g. that of Hsp90N/Cdc37, as hinted at by SEC (Figure 4E), might be expected to not be observed by this method. The results of this experiment are consistent with the data from SEC and, collectively, they indicate that both the N-terminal domain and charged linker region of Hsp90 are required for the interaction with full-length Cdc37.

Interestingly, however, the gel analysis showed that both Hsp90NL and Hsp90NLM interact more weakly with Cdc37 than does the full-length protein, suggesting that the C-terminal domain also plays a role in the interaction with Cdc37. The C-terminal domain of Hsp90 is responsible for the dimerisation of the protein and these results suggest that Cdc37, which is also dimeric, interacts with the full length Hsp90 dimer more favourably than it does with monomeric Hsp90NL and Hsp90NLM.

Solution structure of Hsp90 and the Cdc37/Hsp90 complex

Small angle X-ray scattering (SAXS) is a powerful technique for structural analysis (albeit at low resolution) of proteins in solution. It is well known that the SAXS pattern is sensitive to the size and shape of a scattering molecule.[42] The latter can be estimated using the radius of gyration (R_g) along with its maximum diameter (D_{max}). In this study we carried out SAXS measurements of Cdc37, its Hsp90-binding domain (Cdc37c), Hsp90

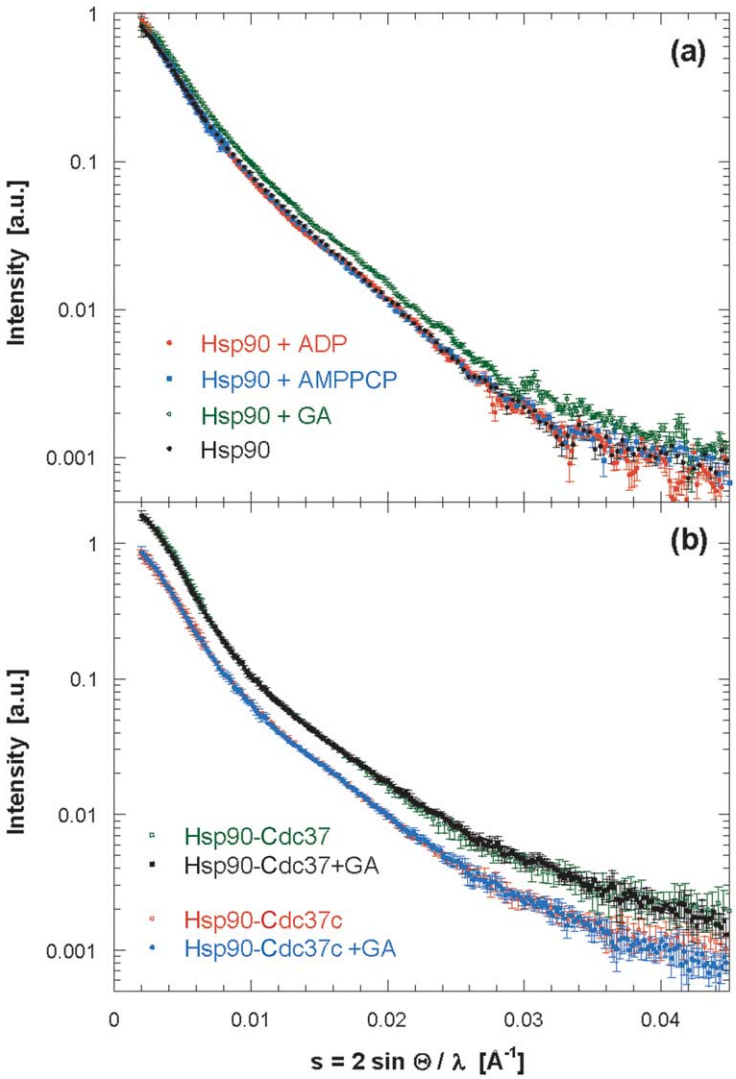

Figure 7. Small-angle X-ray scattering of Hsp90 and Hsp90–Cdc37 complexes. X-ray solution scattering profiles with error bars for: (a) Hsp90 in the presence or absence of either nucleotide or geldanamycin (GA); and (b) Hsp90–Cdc37/Cdc37c complexes with and without GA. All samples have been colour-coded and labelled accordingly. For clarity the profiles for Hsp90–Cdc37 ± GA have been shifted along the vertical axis.

with and without nucleotides and the anti-tumour agent geldanamycin (GA), as well as of complexes between Hsp90 and Cdc37/Cdc37c in the presence and absence of GA. The structural parameters R_g and D_{max} deduced from the scattering profiles for these proteins and protein complexes (see Figure 7) are compiled in Table 1.

Table 1. Structural parameters from solution X-ray scattering analysis

Protein	R_g (Å)	D_{max} (Å)
Cdc37c	16.7	59
Cdc37	43.4	150
Hsp90	64.6	219
Hsp90 + ADP	63.6	218
Hsp90 + AMP-PCP	63.3	210
Hsp90 + GA	56.7	188

	Without GA		With GA	
Protein/complex	R_g (Å)	D_{max} (Å)	R_g (Å)	D_{max} (Å)
Hsp90	64.6	219	56.7	188
Hsp90–Cdc37c	63.3	201	66.4	245
Hsp90–Cdc37	62.7	200	65.1	225

Errors in the experimental values for radius of gyration (R_g) and maximum molecular dimension (D_{max}) are of the order of 1% and 5%, respectively.

Consistent with the fact that the protein was studied at a concentration well above its K_d, the scattering results for full-length Cdc37 clearly indicate that it is a non-compact, dimeric molecule. This conclusion was made by comparing the relative I_o/c values (c = sample concentration) with proteins of known molecular mass and shape. By contrast, the Cdc37c fragment can be characterised as a monomer with compact shape, substantiating our findings made using SEC. Taken together, these results indicate that dimerisation of Cdc37 is not driven by the Hsp90-binding domain and suggest that polypeptide segments outside this domain are likely to be important for dimer formation.

Studies of Hsp90, in its nucleotide-free, ADP- and AMPPCP- (a non-hydrolysable analogue of ATP) bound states were performed next. Interestingly, the results showed that the scattering profile (see Figure 7a), and therefore the solution structure, of Hsp90 does not change dramatically from

that of free hsp90 when different nucleotides are bound. These results are surprising given that ATP-binding and hydrolysis have been proposed to cause significant changes in the conformation of Hsp90.[43] By contrast, the measurements of Hsp90 with and without GA (see Figure 7a) clearly point to a conformational shift in going from a less compact nucleotide-free Hsp90 molecule to a more compact molecule in the GA-bound state, as also indicated by a substantial reduction of R_g and D_{max} (see Table 1). Notably, the binding of ADP does not seem to have a similar effect. Because GA is known to bind to the nucleotide binding site of the N-terminal domain of Hsp90[39,40] these results suggest that GA positively affects the interactions of the two N-terminal domains and thus the overall structure of the Hsp90 dimer. It was originally proposed that GA binds Hsp90 in an ADP-like conformation[39,40] to stabilise an "open" conformation of Hsp90. These results suggest that this may not be the case and that GA instead stabilises a more compact or "closed" conformation.

Interestingly, similar scattering studies of the complexes between Hsp90 and either intact Cdc37 or Cdc37c indicated that the potent influence of GA on the conformation of Hsp90 is abrogated when either full-length Cdc37 or its Hsp90-binding domain (Cdc37c) are bound (see Figure 7b). These results are consistent with the biochemical experiments that suggest that the binding of a Cdc37 dimer locks the two N-terminal domain/linker regions in an Hsp90 dimer into a single conformation. Because the same effect is observed with both the Cdc37c fragment and intact Cdc37, the results confirm that Cdc37c likely contributes most of the interaction surface between Cdc37 and Hsp90. Furthermore, both intact Cdc37 and Cdc37c appear to induce a small decrease in the overall size of the two complexes compared to nucleotide-free Hsp90 (see Table 1), which is consistent with Hsp90 having a more compact structure when bound to its co-chaperone. Although the similarity in the scattering profiles in the presence or absence of GA (of both the Hsp90–Cdc37 and Hsp90–Cdc37c complexes) clearly indicated that the inhibitor has little effect on the structures (see Figure 7b), the derived R_g and D_{max} values (see Table 1) did show an increase in the presence of GA. However, the R_g and D_{max} values are affected by the scattering behaviour at very low angles ($s < 0.008$ Å^{-1}) and their increased size in the presence of GA probably reflects a small amount of aggregation of both Hsp90–Cdc37 complexes in the presence of the inhibitor.

Regulation of Hsp90 ATPase activity by Cdc37 and Cdc37c

Binding and hydrolysing ATP in the N-terminal domains are essential for Hsp90 function *in vivo* and *in vitro*.[5–7] Pearl and co-workers have also shown that the ATPase activity of yeast Hsp90 is down-regulated by human Cdc37.[12] Here, we investigated whether Cdc37 modulates the ATPase activity of human Hsp90. To address this, the ATPase activity of human Hsp90 was measured in both the presence and absence of Cdc37/Cdc37c using a sensitive assay for the detection of inorganic phosphate.[44] p23, a Hsp90 co-chaperone with known inhibitory ATPase activity,[10] was employed as a control. Figure 8 shows that the ATPase activity of Hsp90 was reduced in the presence of a tenfold molar excess of either Cdc37 or Cdc37c, in a similar manner to that of p23. However, the Hsp90 ATPase activity was reduced twofold more in the presence of Cdc37c than it was by the full-length Cdc37, in agreement with the observation that Cdc37c binds more tightly than full-length Cdc37 to the N-terminal domain of Hsp90.

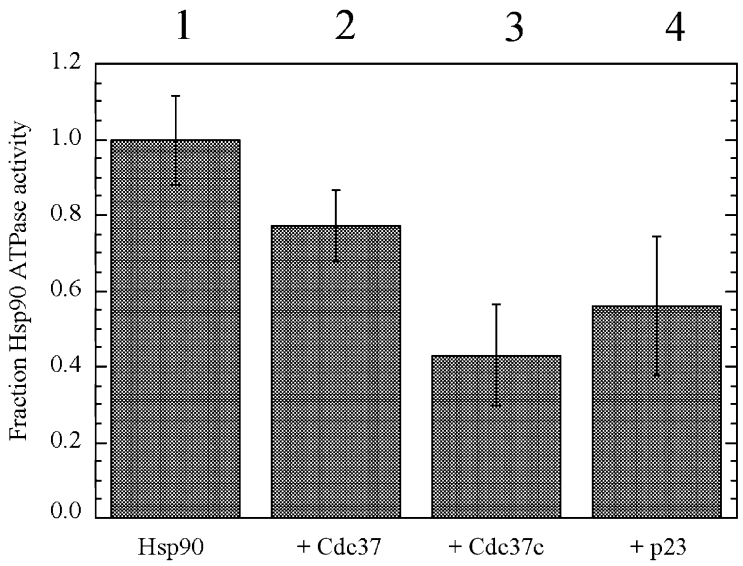

Figure 8. Inhibition of Hsp90 ATPase activity by Cdc37 and Cdc37c. The ATPase activity of human Hsp90β (4 μM) with or without addition of co-chaperones. Lane 1, Hsp90 alone. Lane 2, Hsp90 in the presence of a tenfold molar excess of Cdc37. Lane 3, Hsp90 in the presence of a tenfold molar excess of Cdc37c. Lane 4, Hsp90 in the presence of a fivefold molar excess of p23.

Discussion

We report here a biochemical analysis of the interaction of human Cdc37 and Hsp90β *in vitro*. In agreement with a sequence alignment-derived prediction[29] as well as a recent study[31], limited proteolysis revealed that Cdc37 contains three defined domains. The central region of the protein, residues 147–276, is a structurally stable domain, which is resistant to proteolytic digestion. Residues in the N and C-terminal regions (residues 1–146 and 277–378, respectively) are much less resistant to proteolytic cleavage, an indication that these two regions have a less compact structure. In addition, limited proteolysis of the Cdc37–Hsp90 complex revealed that this central domain of Cdc37, referred to here as Cdc37c, is responsible for the physical interaction with Hsp90. This identified Hsp90-binding domain is some 27 residues shorter than that defined previously (residues 127–283),[31] probably because the proteins were digested under more stringent conditions in our study (non-specific enzyme and incubation at room temperature for up to 1.5 hours). This approach allowed us to identify the minimal structural domain of Cdc37 that is required for binding to Hsp90, which we have subsequently crystallised (M.H. and W.Z., unpublished results). SEC, AUC and SAXS studies showed that the intact Cdc37 protein forms a dimer with a K_d of around 80 μM whereas Cdc37c, the Hsp90-binding domain, is monomeric in solution. This suggests that regions outside of the Hsp90-binding domain are important for the dimerisation of Cdc37.

Using fluorescence spectroscopy we determined that the *in vitro* binding affinity between intact Cdc37 and human Hsp90 (high protein, low salt concentrations) has a K_d of about 4.0 μM. This is consistent with an earlier study, which showed that yeast Hsp90 binds human Cdc37 slightly more tightly[12] than we find the human Hsp90 does. Identification of the Cdc37-binding domain in Hsp90 using SEC and non-denaturing PAGE analysis showed that Cdc37 interacts with the N-terminal domain and charged linker region of Hsp90. These results were also supported by the limited proteolysis experiments, which showed that the N-terminal domain and charged linker region are protected from enzyme digestion when in a complex with Cdc37.

As discussed in Introduction, an earlier study suggested that Cdc37 binds to a site at the C terminus of Hsp90, adjacent to the TPR binding site, because Hop was able to compete with the binding of Cdc37 to Hsp90.[33] However, we could not identify any interaction of either Cdc37 or Cdc37c with the middle plus C-terminal domain construct of Hsp90. Recently, however, it has been shown that Hop binds not only to the C-terminal TPR domain binding site, but also to the N-terminal domain of Hsp90.[13] Thus, the earlier observation that Hop competes with Cdc37 for binding to Hsp90[33] appears to be due to competition for binding to the N-terminal rather than C-terminal regions of Hsp90. In addition, it has also been shown that Cdc37 can interact directly with yeast Hop, which may also be the basis of the observed binding competition to Hsp90.[45]

Limited proteolysis of the Cdc37–Hsp90 complex and Hsp90 alone were very similar to each other, suggesting that the binding of Cdc37 does not cause major structural rearrangements in either Hsp90 or Cdc37. Using native state mass spectrometry we found that a Cdc37 dimer interacts with an Hsp90 dimer. This result is consistent with the non-denaturing PAGE analysis, which showed that the C-terminal domain of Hsp90, which is responsible for dimerisation of Hsp90,[36,46,47] increases the binding of Cdc37. This presumably occurs because in an Hsp90 dimer the local concentration of the two N-terminal domain/linker regions is increased, thereby favouring binding of a Cdc37 dimer.

Small angle X-ray scattering studies of Cdc37, Cdc37c and their complexes with Hsp90 confirmed and extended these conclusions. As discussed above, the SAXS studies confirmed that intact Cdc37 is dimeric, whereas Cdc37c, the Hsp90-binding domain, is monomeric. The SAXS studies also showed that GA, a natural product inhibitor, significantly affects the structure of Hsp90 dimers in solution, producing a more compact shape. Due to the nature of solution X-ray scattering experiments, we have not thus far been able to distinguish between a mixture of conformations or a unique conformation of Hsp90 dimers in solution. However, bearing in mind the limited proteolysis studies presented here and elsewhere,[39] which suggest the presence of flexible linker regions in Hsp90 connecting the N-terminal/middle domains and the middle/C-terminal domains, it is most likely that our derived structural parameters are representative of a mixture or equilibrium of conformational states. Nevertheless, the change of structural quantities such as R_g and D_{max} indicates a clear shift in the equilibrium, i.e. moving from one ensemble of conformations to another with different structural characteristics.

It has been shown by structural and biochemical analysis that the N-terminal domains of Hsp90 contain sites for ATP binding and hydrolysis[40,48] that are crucial for Hsp90 function *in vitro* and *in vivo*. ATP-binding and hydrolysis by Hsp90 are believed to be coupled to conformational changes that lead to the transient association (dimerisation) of the two N-terminal domains in the dimeric Hsp90.[43,49] GA binds to the ATP-binding site in the N-terminal domains of Hsp90. Although we could not demonstrate that binding of either ADP or an ATP analogue affect the structure of Hsp90 (suggesting that they have a more minor effect), the SAXS experiments did suggest that GA favourably influences the interactions between the two adjacent N-terminal domains in an Hsp90 dimer to produce a more compact shape. Most interestingly, binding of either intact Cdc37 or Cdc37c

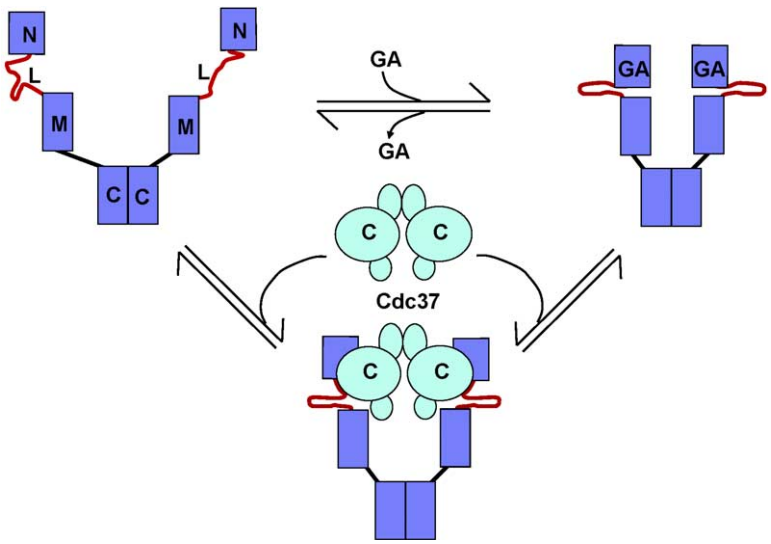

Figure 9. Model for the interaction of Hsp90 with Cdc37 and the mechanism of inhibition of Hsp90 ATPase activity. Each subunit in the Hsp90 homodimer consists of three domains: an N-terminal nucleotide binding domain (N); a middle domain (M), which is separated by a flexible charged linker region (L); and a C-terminal dimerisation domain (C). The current model for the mechanism of ATP hydrolysis by Hsp90 proposes that transient association of the N domains and intra-subunit N and M domain interactions are important for activity.[38] Upon binding either ADP or ATP, Hsp90 adopts a range of conformational states due to the inherent inter-domain flexibility. Geldanamycin (GA), which binds to the ATP binding site, locks Hsp90 into a more compact and inhibited conformation. A Cdc37 dimer interacts with the two N/L domains *via* its central (c) domains and also prevents N-terminal domain interactions critical for ATP hydrolysis.

abrogated this effect of GA. This result suggests that when Cdc37 binds Hsp90 it locks the conformation of the two Hsp90 N-terminal domains in one position preventing an effect by GA on the Cdc37–Hsp90 complex. This conclusion is consistent with the biochemical experiments, where binding of a Cdc37 dimer to the two N-terminal domain/linker regions in Hsp90 would be expected to lock the N-terminal domains in a particular conformation. It is also consistent with the small decrease in overall size of both the Hsp90–Cdc37 and Hsp90–Cdc37c complexes, compared to free Hsp90, which further indicate that Hsp90 has reduced conformational flexibility when bound to its co-chaperone. Finally, because both intact Cdc37 and Cdc37c have the same effect in the SAXS studies reported here, it is likely that Cdc37c provides most of the interaction surface with Hsp90.

These results of our work when considered together suggest a model for the interaction of Cdc37 with Hsp90 (see Figure 9), whereby a Cdc37 dimer binds the two N-terminal domain/charged linker regions in an Hsp90 dimer, fixing them in a single conformation. This mode of binding nicely explains all the experimental results that we have observed. In particular, it explains why the C-terminal domain of Hsp90 enhances, by stabilisation of the Hsp90 dimer, the binding of Cdc37. Moreover, it also explains why the binding of Cdc37 inhibits the ATPase activity of Hsp90, because binding of Cdc37 inhibits the proposed ATPase cycle of Hsp90 by fixing the N-terminal domains of Hsp90 in a particular conformation. In considering this model it should be noted that in both our own and previous studies[12] the K_d for dimerisation of Cdc37 is lower than that for Cdc37–Hsp90 assembly. This suggests that Cdc37 may not assemble on to Hsp90 as a pre-formed dimer (as shown for clarity in Figure 9), but that instead the binding of Cdc37 to Hsp90 (which has greater affinity) may promote Cdc37 dimerisation.

In addition to the N-terminal domain the charged linker region of Hsp90, which is the least conserved part of Hsp90, is also required for the association of Cdc37. This region has been shown to have a role in modulating the nucleotide binding affinity of the N-terminal domain,[50] and it is believed that it provides a hinge that allows the two N-terminal domains to open and close during the hydrolysis of ATP and when releasing or reloading client protein substrates. Binding of Cdc37 to the charged linker region, in addition to the N-terminal domains, might also help to restrict the movement of N-terminal domains, which are directly clamped in one conformation by their binding to Cdc37. The SAXS studies suggest that the structure of the resulting Cdc37–Hsp90 complex is intermediate in compactness between that of the isolated Hsp90 and the more compact Hsp90–GA complex.

As mentioned above, in the Hsp90-dependent steroid hormone receptor pathway, Sti1, the yeast analogue of human Hop, has been shown to interact with both the N and C-terminal regions of Hsp90.[13] The interaction site in the N terminus of Hsp90 is within the first 24 amino acid residues, a region that has also been suggested to be important for N-terminal domain dimerisation.[49] Cdc37 and Hop/Sti1 share many common features; both play a role as scaffold proteins in the recruitment of client protein substrates, both are dimers, and both directly interact with Hsp90 in a salt-dependent manner.[13,28] However, most importantly, both are inhibitors of the Hsp90 ATPase activity.[12,13] Buchner *et al*.[13] have proposed that one of the

functions of Sti1/Hop is to regulate the Hsp90 ATPase activity by preventing the association of the N-terminal domains. Our work suggests that Cdc37 shares this mechanism. Future work needs to address how Cdc37 binding and inactivation of Hsp90, shown here, helps recruit client proteins onto Hsp90 for subsequent activation.

After this manuscript had been completed, Roe *et al*.[51] published the crystal structure of a complex of the C-terminal fragment of human Cdc37 (residues 138–378) bound to the N-terminal domain of yeast Hsp90 (residues 1–208). The conclusions that they draw from their work are broadly similar to our own, although we find that both the N-terminal domain plus the adjacent charged linker region of human Hsp90β are required for the interaction with intact Cdc37. In addition, in the crystal structure Cdc37 forms homodimeric contacts with a symmetry-related molecule in the crystal; these interactions all involve residues, e.g. a helix-loop-helix motif (residues 240–254), which are present in our Hsp90-binding fragment, Cdc37c. However, our studies point to this Cdc37c fragment being monomeric in solution and suggest instead that residues outside the Cdc37c domain are required for dimerisation. Further experiments, and very likely the structure of the complex of Cdc37 with human Hsp90, will be needed to understand these observed differences.

Materials and Methods

Plasmid construction

Full-length human Cdc37[19] and human Hsp90β in a pET14b vector were used as templates in the polymerase chain reactions described below. To construct Cdc37c, the region encoding the central domain of human Cdc37 (amino acid residues 147–276) was amplified using a forward primer 5′-CCGGGATCCAAACACAAGACCTTC-3′ and a reverse primer 5′-CGCGAATTCTCACTTCATG GCCTTCTC-3′. The PCR fragment was cloned in-frame between the BamHI/EcoRI sites of the pGEX-2T vector (Pharmacia). For the construction of Hsp90NL, the DNA fragment encoding the N-terminal domain plus charged linker region (amino acid residues 4–261) of Hsp90 was amplified using a forward primer (N1) 5′-CCGGGATCC GTGCACCATGGAGAGGAG-3′ and a reverse primer 5′-CGCGAATTCTCAACCGCTGTCATCCTCCTC-3′. For the construction of Hsp90N, the region encoding the N-terminal domain (amino acid residues 1–222) of Hsp90 was amplified with the forward primer 5′-CCGG GATCCCCTGAGGAAGTGCACCAT-3′ and a reverse primer 5′-CGCGAATTCTCACTTCTCTCGTTCCTT-3′. The PCR fragments of Hsp90NL and Hsp90N were both cloned into the BamHI/EcoRI sites of the pGEX-2T vector. For the construction of Hsp90NLM, the sequence encoding the N-terminal domain, charged linker and middle domain (amino acid residues 4–576) was amplified with a forward primer 5′CCGGGATCCCATATGGT GCACCATGGAGAGGAG-3′ and a reverse primer 5′-CGGCTCGAGTCACTTCTCAACCTTCTTATC-3′. The PCR fragment was cloned into the NdeI/XhoI sites of the pET16b vector (Novagen). For the construction of Hsp90MC, the sequence encoding the middle and C-terminal domains (amino acid residues 275–723) was amplified with a forward primer 5′-GCACAGCCGCA TATGGGATCCTACATTGATCAGGAA-3′ and a reverse primer 5′-GCGAGATCTTTAATCGACTTCTTCCATGCA-3′. The PCR fragment was digested with NdeI/BglII and cloned into the NdeI/BamHI sites of the pET16b vector. All the constructs were verified by DNA sequencing.

Protein expression and purification

All full-length proteins and their truncated variants were expressed in *E. coli* strain BL21(DE3) at 37 °C in LB media and induced with 0.4 mM isopropyl-thiogalactoside (IPTG). The cells were lysed by sonication in buffer A: 25 mM Tris–HCl (pH 8.0), 100 mM NaCl, 1 mM dithiothreitol (DTT). The insoluble cell debris was removed by centrifugation. For purification of glutathione-*S*-transferase (GST) fusion proteins, the cleared supernatant was applied to glutathione–agarose resin (Amersham Pharmacia Biotech) which was pre-equilibrated with buffer A. The unbound proteins were removed by washing with buffer A and the bound GST-fusion proteins were eluted with buffer A containing 10 mM reduced glutathione (Sigma). The eluted fusion proteins were buffer-exchanged into thrombin cleavage buffer: 50 mM Tris–HCl (pH 8.4), 150 mM NaCl, 2.5 mM $CaCl_2$ by dialysis. GST was cleaved from the fusion protein with thrombin, at a ratio of one unit of enzyme per milligram of fusion protein at room temperature for two hours. Subsequently, GST was separated from the protein of interest by anion exchange chromatography on a Mono Q HR10/10 column (Amersham Pharmacia Biotech) with a linear gradient of 0–1 M NaCl in Tris–HCl (pH 8.0) buffer over 180 ml. The pooled protein fractions were further purified by gel filtration on a Superdex 200 HR 16/60 column (Amersham Pharmacia Biotech) in 25 mM Tris–HCl (pH 8.0) 25 mM NaCl, 1 mM DTT. Fractions containing protein were pooled, concentrated and either immediately used for the experiments or stored at −80 °C. For the His-tagged full-length or truncated variants of human Hsp90, the purification procedure was similar to that of the GST fusions described above. However, in this case the cleared supernatants were applied to a Ni^{2+}-NTA affinity resin (Qiagen), washed with buffer A, eluted with buffer A containing 250 mM imidazole, and purified using a combination of anion exchange chromatography on a Mono Q HR10/10 column and size-exclusion chromatography on a Superdex 200 HR 16/60 column. Expression and purification of human p23 protein was described by McLaughlin *et al*.[10]

Determination of K_d using fluorescence spectroscopy

Binding of increasing concentrations of Cdc37 (0–70 μM) to (15 μM) human Hsp90 in 25 mM Tris–HCl (pH 8.0), and 25 mM NaCl was monitored by fluorescence spectroscopy with excitation at 280 nm and emission at 340 nm using a Perkin–Elmer LS55 spectrofluorimeter in a 1 cm path length cuvette. The final titration volume was less than 15% of the initial volume. The fluorescence of increasing concentrations of Cdc37 was also monitored and the fluorescence change (ΔF) of Cdc37 on binding to Hsp90 was calculated by subtracting the two sets of titrations. Using a single-binding site model, where the concentration of the Cdc37–Hsp90

complex is directly proportional to the change in fluorescence (ΔF), the data where fitted to the following equation:

$$\Delta F = [L]\Delta F_{max}/([L] + K_d) \quad (1)$$

where $[L]$ is Cdc37 concentration and K_d is the dissociation constant. The K_d value was calculated graphically using the KaleidaGraph (Synergy Software, Inc.) software.

Analytical ultracentrifugation (AUC)

Sedimentation equilibrium analysis was performed using a Beckman Optima XL-I analytical ultracentrifuge equipped with absorbance optics, using an An-60Ti rotor at 4 °C. Cdc37 was dialysed against 25 mM Tris–HCl (pH 8.0), 25 mM NaCl, 2 mM Tris (2-carboxyethyl) phosphine, (TECP). Three samples were run simultaneously with initial uniform protein concentrations giving an A_{280} (1 cm path length) of 0.2, 0.3, and 0.5, respectively. Dialysis buffer was used as a blank reference. Data were collected at equilibrium for four different angular velocities: 13,200 rpm, 14,500 rpm, 16,000 rpm and 18,700 rpm. The concentration was measured as a function of radial position and absorbance at 280 nm. Data points were 0.001 cm apart and the final data were an average of five measurements. Data analysis was performed using WinNonlin 1.06.[52] Values for the solvent density and protein partial specific volume of 0.7232 ml/g and 1.00175 ml/g, respectively, were calculated using Sednterp (University of New Hampshire). The K_d obtained from this analysis was calculated based on an extinction coefficient of 50,420 $M^{-1}\,cm^{-1}$ for Cdc37. Only data points with A_{280} values between 0.1 and 1.0 were included in the analysis.

Size-exclusion chromatography (SEC)

Either 20 μl containing a single protein or 40 μl of a mixture of two proteins (at a final protein concentration of 150 μM) were loaded onto a Superdex 200 PC 3.2/30 analytical column (Amersham Pharmacia Biotech) pre-equilibrated with buffer A at 4 °C on a Smart System (Amersham Pharmarcia Biotech). Fractions of 80 μl were collected at a flow-rate of 40 μl/minute, and absorbance was measured at 280 nm.

Polyacrylamide gel electrophoresis

For denaturing conditions, protein samples were heated in SDS and loaded on to 4–12% (w/v) NuPAGE gels and run under the conditions recommended by the manufacturer (Novex). For non-denaturing (native) gels, purified proteins were diluted to a final concentration of 70 μM in buffer A containing 1 mM fresh DTT. Protein samples were incubated on ice for one hour, mixed with native gel loading buffer and loaded on to a 14% Tris–Glycine gel (Novex). The gel was run under non-denaturing (native) conditions, following the recommendation of the manufacturer (Novex). Both denaturing and non-denaturing gels were stained with Coomassie Brilliant Blue.

Limited proteolysis

Purified His-tagged Hsp90, non-tagged Cdc37 and Hsp90–Cdc37 complexes were subjected to proteolytic digestion by Subtilisin (Sigma) using 0.5% (w/w) of enzyme-substrate at room temperature in buffer A. At each time point, aliquots of digested samples were boiled in SDS-loading buffer to stop the reaction and analysed on a 4–12% NuPAGE gel.

ATPase assay

ATPase activities of 4 μM purified human Hsp90β in the absence or in the presence of 40 μM of Cdc37 or Cdc37c or 20 μM of p23 were measured using a fluorescence-based assay involving the phosphate binding protein as described.[10,44] All activities are the averages of three or more separate experiments.

Small-angle X-ray scattering experiments (SAXS)

SAXS data were collected at three different synchrotron radiation facilities, at beamline ID02 of the ESRF[53] at beamline BL45XU of SPring-8[54] and at station 2.1 of the Daresbury SRS.[55] Whereas the former two are optimized for an X-ray wavelength of 1 Å, the camera at SRS station 2.1 is operated at a wavelength of 1.54 Å. CCD detectors with X-ray image intensifiers are in use at beamlines BL45XU and ID02. Station 2.1 is equipped with a gas-filled 2D wire chamber. On all three SAXS cameras the intensity of the incident X-rays was monitored by an ionisation chamber installed in front of the sample which was contained in a beamline-specific standard sample cell. Protein concentrations of 4 mg/ml were used in the presence or absence of nucleotide or inhibitors at least five times the concentration of the binding constants. Reduction of the 2D-SAXS patterns of samples and corresponding buffers to 1D scattering profiles was performed using established procedures developed and available at each of the three beamlines. Due to the high X-ray flux from the two third-generation synchrotron sources, the data acquisition time was divided in frames of 1 second compared to 60 seconds at station 2.1 of the Daresbury SRS in order to monitor radiation damage (buffer and sample were measured in alternation). Sample-to-detector distances were configured so as to cover the low angle region characterised by the momentum transfer interval of $0.002\ Å^{-1} \le s \le 0.045\ Å^{-1}$ for all three experimental setups. The modulus of the momentum transfer is defined as $s = 2\sin\Theta/\lambda$, where 2Θ is the scattering angle. Reduction and analysis of 1D scattering data sets were performed as described.[56] Radius of gyration (R_g), forward scattering intensity (I_o) and the intraparticle distance distribution function $p(r)$ were calculated from the experimental scattering data using the indirect Fourier transform method as implemented in the program GNOM.[57] The maximum linear dimension D_{max} of the particle can be evaluated owing to the characteristic of $p(r)$. In order to check the consistency of the results radii of gyration were also determined from the very low angle profiles by using the Guinier analysis based on the approximation:

$$\ln I(s) = \ln I_o - 4\pi^2 R_g^2 s^2/3 \quad (2)$$

Acknowledgements

We thank Dr L. Brizuela (Harvard Medical

School, Cambridge, USA) for the pGEX-Cdc37 plasmid, Dr M. Shirouzu, Dr Y. Ito and Professor S. Yokoyama (RIKEN Genomic Sciences Center, Yokohama, Japan) for the pET14b-Hsp90 plasmid and Dr L. Packman, R. Turner and M. Weldon at the PNAC facility for mass spectrometry and N-terminal sequencing. The SAXS experiments at ESRF and SPring-8 were carried out with the assistance of Dr S. Finet (ESRF) and Drs T. Fujisawa and S. Akiyama (SPring-8). S.H.M. was funded, in part, by the Welton Foundation and a Leverhulme Trust Special Research Fellowship, whilst G.A.L. was funded by a fellowship from The Jane Coffin Childs Memorial Fund for Medical Research. This work was supported by grants from the BBSRC and the EU (Contract No: QLK3-1999-00875).

References

1. Pratt, W. B. (1998). The hsp90-based chaperone system: involvement in signal transduction from a variety of hormone and growth factor receptors. *Proc. Soc. Exp. Biol. Med.* **217**, 420–434.
2. Richter, K. & Buchner, J. (2001). Hsp90: chaperoning signal transduction. *J. Cell Physiol.* **188**, 281–290.
3. Picard, D. (2002). Heat-shock protein 90, a chaperone for folding and regulation. *Cell Mol. Life Sci.* **59**, 1640–1648.
4. Young, J. C., Moarefi, I. & Hartl, F. U. (2001). Hsp90: a specialized but essential protein-folding tool. *J. Cell. Biol*, **154**, 267–273.
5. Panaretou, B. (1998). ATP binding and hydrolysis are essential to the function of the Hsp90 molecular chaperone *in vivo*. *EMBO J.* **17**, 4829–4836.
6. Obermann, W. M., Sondermann, H., Russo, A. A., Pavletich, N. P. & Hartl, F. U. (1998). *In vivo* function of Hsp90 is dependent on ATP binding and ATP hydrolysis. *J. Cell Biol.* **143**, 901–910.
7. Grenert, J. P., Johnson, B. D. & Toft, D. O. (1999). The importance of ATP binding and hydrolysis by Hsp90 in formation and function of protein heterocomplexes. *J. Biol. Chem.* **274**, 17525–17533.
8. Scheibel, T., Weikl, T. & Buchner, J. (1998). Two chaperone sites in Hsp90 differing in substrate specificity and ATP dependent. *Proc. Natl Acad. Sci. USA*, **95**, 1495–1499.
9. Prodromou, C., Siligardi, G., O'Brien, R., Woolfson, D. N., Regan, L., Panaretou, B. *et al.* (1999). Regulation of Hsp90 ATPase activity by tetratricopeptide repeat (TPR)-domain co-chaperones. *EMBO J.* **18**, 754–762.
10. McLaughlin, S. H., Smith, H. W. & Jackson, S. E. (2002). Stimulation of the weak ATPase activity of human hsp90 by a client protein. *J. Mol. Biol.* **315**, 787–798.
11. Panaretou, B., Siligardi, G., Meyer, P., Maloney, A., Sullivan, J. K. & Singh, S. (2002). Activation of the ATPase activity of Hsp90 by the stress-regulated cochaperone Aha1. *Mol. Cell*, **10**, 1307–1318.
12. Siligardi, G., Panaretou, B., Meyer, P., Singh, S., Woolfson, D. N., Piper, P. W. *et al.* (2002). Regulation of Hsp90 ATPase activity by the co-chaperone Cdc37p/p50cdc37. *J. Biol. Chem.* **277**, 20151–20159.
13. Richter, K., Muschler, P., Hainzl, O., Reinstein, J. & Buchner, J. (2003). Sti1 is a non-competitive inhibitor of the Hsp90 ATPase. *J. Biol. Chem.* **278**, 10328–10333.
14. Russell, L. C., Whitt, S. R., Chen, M.-S. & Chinkers, M. (1999). Identification of conserved residues required for the binding of a tetratricopeptide repeat domain to heat shock protein 90. *J. Biol. Chem.* **274**, 20060–20063.
15. Smith, D. F. (1993). Dynamics of heat-shock protein 90-progesterone receptor-binding and the disactivation loop model for steroid–receptor complexes. *Mol. Endocrin.* **7**, 1418–1429.
16. Nicolet, C. M. & Craig, E. A. (1989). Isolation and characterisation of STI1, a stress-inducible gene from *Saccharomyces cerevisiae*. *Mol. Cell. Biol.* **9**, 3000–3008.
17. McLean, M. & Picard, D. (2003). Cdc37 goes beyond Hsp90 and kinases. *Cell Stress Chaperones*, **8**, 114–119.
18. Dai, K., Kobayashi, R. & Beach, D. (1996). Physical interaction of mammalian CDC37 with CDK4. *J. Biol. Chem.* **271**, 22030–22034.
19. Lamphere, L., Fiore, F., Xu, X., Brizuela, L., Keezer, S., Sardet, C., Draetta, G. F. & Gyuris, J. (1997). Interaction between Cdc37 and Cdk4 in human cells. *Oncogene*, **14**, 1999–2004.
20. Mahony, D., Parry, D. A. & Lees, E. (1998). Active cdk6 complexes are predominantly nuclear and represent only a minority of the cdk6 in T cells. *Oncogene*, **16**, 603–611.
21. O'Keeffe, B., Fong, Y., Chen, D., Zhou, S. & Zhou, Q. (2000). Requirement for a kinase-specific chaperone pathway in the production of a Cdk9/cyclin T1 heterodimer responsible for P-TEFb-mediated tat stimulation of HIV-1. *J. Biol. Chem.* **275**, 279–287.
22. Tzivion, G., Luo, Z. & Avruch, J. (1998). A dimeric 14-3-3 protein is an essential cofactor for Raf kinase activity. *Nature*, **394**, 88–92.
23. Grammatikakis, N., Lin, J. H., Grammatikakis, A., Tsichlis, P. N. & Cochran, B. H. (1999). p50(cdc37) acting in concert with Hsp90 is required for Raf-1 function. *Mol. Cell. Biol.* **19**, 1661–1672.
24. Basso, A. D., Solit, D. B., Chiosis, G., Giri, B., Tsichlis, P. & Rosen, N. (2002). Akt forms an intracellular complex with Hsp90 and Cdc37 and is destabilized by inhibitors of Hsp90 function. *J. Biol. Chem.* **277**, 39858–39866.
25. Fliss, A. E., Fang, Y., Boschelli, F. & Caplan, A. J. (1997). Differential *in vivo* regulation of steroid hormone receptor activation by cdc37p. *Mol. Cell. Biol.* **8**, 2501–2509.
26. Wang, X., Grammatikakis, N. & Hu, J. (2002). Role of p50/CDC37 in Hepadnavirus assembly and replication. *J. Biol. Chem.* **277**, 24361–24367.
27. Stepanova, L., Leng, X., Parker, S. B. & Harper, J. W. (1996). Mammalian p50Cdc37 is a protein kinase-targeting subunit of Hsp90 that binds and stabilizes Cdk4. *Genes Dev.* **10**, 1491–1502.
28. Hartson, S. D., Irwin, A. D., Shao, J., Scroggins, B. T., Volk, L., Huang, W. & Matts, R. L. (2000). p50(cdc37) is a nonexclusive Hsp90 cohort which participates intimately in Hsp90-mediated folding of immature kinase molecules. *Biochemistry*, **39**, 7631–7644.
29. Shao, J., Grammatikakis, N., Scroggins, B. T., Uma, S., Huang, W., Chen, J. J., Hartson, S. D. *et al.* (2001). Hsp90 regulates p50(cdc37) function during the biogenesis of the active conformation of the heme-regulated eIF2 alpha kinase. *J. Biol. Chem.* **276**, 206–214.
30. Lee, P., Rao, J., Fliss, A., Yang, E., Carrett, S. & Caplan, A. J. (2002). The Cdc37 protein kinase-binding domain is sufficient for protein kinase activity and cell viability. *J. Cell Biol.* **159**, 1051–1059.
31. Shao, J., Irwin, A., Hartson, S. D. & Matts, R. L.

(2003). Function dissection of Cdc37: characterisation of domain structure and amino acid residues critical for protein kinase binding. *Biochemistry*, **42**, 12577–12588.
32. Scholz, G. M., Cartledge, K. & Hall, N. E. (2001). Identification and characterization of Harc, a novel Hsp90-associating relative of Cdc37. *J. Biol. Chem.* **276**, 30971–30979.
33. Silverstein, A. M., Grammatikakis, N., Cochran, B. H., Chinkers, M. & Pratt, W. B. (1998). p50(cdc37) binds directly to the catalytic domain of Raf as well as to a site on hsp90 that is topologically adjacent to the tetratricopeptide repeat binding site. *J. Biol. Chem.* **273**, 20090–20095.
34. Grammatikakis, N., Vultur, A., Ramana, C. V., Siganou, A., Schweinfest, C. W., Watson, D. K. & Raptis, L. (2002). The role of Hsp90N, a new member of the Hsp90 family, in signal transduction and neoplastic transformation. *J. Biol. Chem.* **277**, 8312–8320.
35. Maruya, M., Sameshima, M., Nemoto, T. & Yahara, I. (1999). Monomer arrangement in HSP90 dimer as determined by decoration with N and C-terminal region specific antibodies. *J. Mol. Biol.* **285**, 903–907.
36. Nemoto, T., Ohara-Nemoto, Y., Ota, M., Takagi, T. & Yokoyama, K. (1995). Mechanism of dimer formation of the 90-kDa heat-shock protein. *Eur. J. Biochem.* **233**, 1–8.
37. Nemoto, T., Sato, N., Iwanari, H., Yamashita, H. & Takagi, T. (1997). Domain structures and immunogenic regions of the 90-kDa heat-shock protein (HSP90). Probing with a library of anti-HSP90 monoclonal antibodies and limited proteolysis. *J. Biol. Chem.* **272**, 26179–26187.
38. Meyer, P., Prodromou, C., Hu, B., Vaughan, C., Roe, S. M., Panaretou, B. *et al.* (2003). Structural and functional analysis of the middle segment of hsp90: implications for ATP hydrolysis and client protein and cochaperone interactions. *Mol. Cell.* **11**, 647–658.
39. Stebbins, C. E., Russo, A. A., Schneider, C., Rosen, N., Hartl, F. U. & Pavletich, N. P. (1997). Crystal structure of an Hsp90–geldanamycin complex: targeting of a protein chaperone by an antitumor agent. *Cell*, **89**, 239–250.
40. Prodromou, C., Roe, S. M., O'Brien, R., Ladbury, J. E., Piper, P. W. & Pearl, L. H. (1997). Identification and structural characterization of the ATP/ADP-binding site in the Hsp90 molecular chaperone. *Cell*, **90**, 65–75.
41. Wegele, H., Muschler, P., Bunck, M., Reinstein, J. & Buchner, J. (2003). Dissection of the contribution of individual domains to the ATPase mechanism of Hsp90. *J. Biol. Chem.* **278**, 39303–39310.
42. Feigin, L. A. & Svergun, D. I. N. Y. a. L. P. P. (1987). *Structure Analysis by Small-angle X-Ray and Neutron Scattering*, Plenum, New York.
43. Prodromou, C., Panaretou, B., Chohan, S., Siligardi, G., O'Brien, R., Ladbury, J. E. *et al.* (2000). The ATPase cycle of Hsp90 drives a molecular "clamp" *via* transient dimerization of the N-terminal domains. *EMBO J.* **19**, 4383–4392.
44. Brune, M., Hunter, J. L., Howell, S. A., Martin, S. R., Hazlett, T. L., Corrie, J. E. & Webb, M. R. (1998). Mechanism of inorganic phosphate interaction with phosphate binding protein from *Escherichia coli*. *Biochemistry*, **37**, 10370–10380.
45. Abbas-Terki, T., Briand, P. A., Donze, O. & Picard, D. (2002). The Hsp90 co-chaperones Cdc37 and Sti1 interact physically and genetically. *J. Biol. Chem.* **383**, 1335–1342.
46. Minami, Y., Kimura, Y., Kawasaki, H., Suzuki, K. & Yahara, I. (1994). The carboxy-terminal region of mammalian HSP90 is required for its dimerization and function *in vivo*. *Mol. Cell. Biol.* **14**, 1459–1464.
47. Meng, X., Devin, J., Sullivan, W. P., Toft, D., Baulieu, E. E. & Catelli, M. G. (1996). Mutational analysis of Hsp90 alpha dimerization and subcellular localization: dimer disruption does not impede "*in vivo*" interaction with estrogen receptor. *J. Cell Sci.* **109**, 1677–1687.
48. Grenert, J. P., Sullivan, W. P., Fadden, P., Haystead, T. A. J., Clark, J., Mimnaugh, E. *et al.* (1997). The amino-terminal domain of heat shock protein 90 (hsp90) that binds geldanamycin is an ATP/ADP switch domain that regulates hsp90 conformation. *J. Biol. Chem.* **272**, 23843–23850.
49. Richter, K., Reinstein, J. & Buchner, J. (2002). N-terminal residues regulate the catalytic efficiency of the Hsp90 ATPase. *J. Biol. Chem.* **277**, 44905–44910.
50. Scheibel, T., Siegmund, H. I., Jaenicke, R., Ganz, P., Lilie, H. & Buchner, J. (1999). The charged region of Hsp90 modulates the function of the N-terminal domain. *Proc. Natl Acad. Sci. USA*, **96**, 1297–1302.
51. Roe, S., Ali, M., Meyer, P., Vaughan, C., Panaretou, B., Piper, P. *et al.* (2004). The mechanism of Hsp90 regulation by the protein kinase-specific cochaerone p50cdc37. *Cell*, **116**, 87–98.
52. Johnson, M. L., Correia, J. J., Yphantis, D. A. & Halvorson, H. R. (1981). Analysis of data from the analytical ultracentrifuge by nonlinear least-squares techniques. *Biophys. J.* **36**, 575–588.
53. Narayanan, T., Diat, O. & Bösecke, P. (2001). SAXS and USAXS on the high brilliance beamline at the ESRF. *Nucl. Instr. Meth. Phys. Res. A*, **467-468**, 1005–1009.
54. Fujisawa, T., Inoue, K., Oka, T., Iwamoto, H., Uruga, T., Kumasaka, T. *et al.* (2000). Samll-angle X-ray scattering station at Spring-8 RIKEN beamline. *J. Appl. Crystallog.* **33**, 797–800.
55. Townes-Andrews, E., Berry, A., Bordas, J., Mant, G. R., Murray, P. K., Roberts, K. *et al.* (1989). Time-resolved X-ray diffraction station: X-ray optics, detectors, and data acquisition. *Rev. Sci. Instrum.* **60**, 2346–2349.
56. Grossmann, J. G., Hall, J. F., Kanbi, L. D. & Hasnain, S. S. (2002). The N-terminal extension of rusticyanin is not responsible for its acid stability. *Biochemistry*, **41**, 3613–3619.
57. Semenyuk, A. V. & Svergun, D. I. (1991). GNOM—a program package for small-angle scattering data processing. *J. Appl. Crystallog.* **24**, 537–540.

Edited by R. Huber

(Received 19 January 2004; received in revised form 7 May 2004; accepted 11 May 2004)